

Evaluation about Detection of Defects in the Nuclear Piping Loop System Using Lock-in Infrared Thermography

by S. C. KIM *, H. C. JUNG ** and K. S. KIM ***

* Department of Mechanical System Engineering, Chosun University, Gwangju, Korea, bluerune@nate.com

** Department of Mechanical System Engineering, Chosun University, Gwangju, Korea, hyunchul.jung@chosun.ac.kr

*** Department of Mechanical System Engineering, Chosun University, Gwangju, Korea, gsckim@chosun.ac.kr

Abstract

Using lock-in IR thermography, detection conditions of defect in pipeline for nuclear power plant has been studied according to incidence angle. Defects are manufactured by changing length of wall thinning, angle in circumferential direction, and amount of wall thinning. Corresponding pipe with defect is used to build loop pipeline system for nuclear power plant, and lock-in IR thermography for cold defect condition is applied to detect heating defect. IR thermography camera and cooling unit is used, and distance between cooling device and target loop system is set to 2 m away. For the analysis on experimental results, cooling temperature distribution and phase data are gathered to measure the length of defect.

1. Introduction

To prevent wall thinning and damage in pipeline for nuclear power plant, non-destructive test before and during operation is usually implemented. In addition, to shorten the cycle of testing or increase the quality of inspection, test time and cost will be increased significantly. To compensate these shortcomings, many non-destructive testing methods have been developed, and to increase the chance of catching wall thinning and possibility of damage using non-destructive testing is to shorten the cycle of corresponding test. This would be the most important factor to ensure quality. As the number of nuclear power plant operations increases and therefore the power plants are rapidly aging, the use of non-destructive tests, which can be performed relatively safe and quick, is also increasing. In addition, nuclear power plant piping used for a long period of time is subject to various types of deterioration such as fatigue, corrosion, and wall-thinning defect. Among them, the wall-thinning defect caused by low accelerated corrosion is one of major causes that degrade the health of nuclear power plant piping [1, 2]. The wall-thinning defect progresses without any sign of damage and commonly occurs in the base metal as well as in the weld, making it difficult to detect the defect through the conventional operation test. For this reason, nuclear power plants operate a separate wall-thinning defect management program and accordingly carry out wall-thickness test for parts with high possibility of wall-thinning defects [3, 4]. For inspection of the pipe thickness, ultrasonic test is most commonly used but it takes a lot of time since it has to measure the thickness at all lattice points. For pipes with small diameters, radiographic inspection is used but it lacks quantization for defects, has a risk of exposing the inspector to radiation and therefore has a limitation in field application [5, 6]. Among non-contact, non-destructive testing techniques that can detect several wall-thinning defects quickly and simply, Infrared Thermography (IRT) has been studied for application [7, 8]. But IR thermography method is limited to image processing technique, and further improvement, such as micro defect or exact location determination, is needed. To overcome the limitation of thermography, which is usually used to detect temperature change and its post-processing, lock-in mode thermography is developed to obtain precise image. Generally according to the types of defects, light, ultrasound, vibration, eddy current, etc., which can be easily controlled by harmonic function, are used for excitation source according to defect type. In this study, lock-in IR thermography is used to determine test condition for defect identification.

2. Equipment and Objects

2.1 Camera

The camera used for this study is as shown in Fig.1, and its specifications are listed in Table 1. Infrared thermography is a technique that calculates phase and amplitude through digital signal processing with a high resolution (0.02°C) in order to measure minute changes in temperature in a mechanical structure. In this study, preceding experiments were performed in two conditions: First one was to assume that the nuclear power plant was shut down due to regular inspection and the other one was to assume that it was operating normally. In these two conditions, the state of pipes at normal temperature was inspected outside through heat flow of silicon oil inside the pipes. However, in this study, the insulation was not taken into consideration.



Figure 1. Infrared Camera

Table 1. Specification of Infrared Camera

Infrared Camera (FLIR, SC 5200)	
Detector Materials	InSb (Indium Antimonide)
Cooling method	Stirling Cooler
Spectral Response (um)	3.7 ~ 5.0
Number of Pixels	320 × 256
Pitch (um)	30 × 30
NETD	25mK@25℃
Measure range (℃)	-15 ~ 2000
Frame rate(Hz)	5 ~ 400

2.2 Cooling device(Fan)

Fan cooler with better directionality and high speed is used for the study. Wind blower can cool the corresponding specimen via forced convection using the difference between fan inlet and outlet. Also, better directionality can ensure cooling in 2 ~ 3 m away. Fan cooler features aluminum die casting blade, and weight is reduced to 11 kg. Maximum wind speed is 16.5 m/sec, and blade length is 270 mm to ensure uniform cooling on pipe specimen. Fig. 2 shows the picture of fan cooler with high speed blower. According to the distance between pipe and 2 cooling units and the one between pipe and IR thermography camera, the analysis results are reviewed. 70% of rated power is applied on halogen lamp, and cooling lock-in IRT is used for image collection. Cooling cycle is set to 0.1 Hz.



Figure 2. Cooling device

2.3 Heat Flow System

For this study, a loop system as shown in Fig. 3 was made using 2.5-inch pipes of ASTM A106 Gr.B carbon steel, and its specifications are shown in Table 2. In order to simulate a high-temperature pipe system of a normally operating nuclear power plant, the temperature inside the pipes was maintained at 250 using silicon oil. Distance between the cooling device and the pipe was set to 1.5m. Thermal properties of the ASTM A106 Gr.B carbon steel pipe used for this study are shown in Table 2.

Table 2. Specification of piping loop system

Piping Loop system	
Pipe type	2.5 inch Pipe
Operating temperature	T > 250 °C
Pressure	atmospheric pressure
Inside fluid	silicone oil
Pump of capacity	40 l/min
Heater of capacity	20 kW



Figure 3. Loop system and infrared thermography

2.4 Wall-thinned Pipe Specimen

In order to perform this experiment, the pipes made with the materials actually used in a nuclear power plant were used and defects with the following conditions were processed inside the pipes. The 2.5-inch pipe with the thickness (t) of 7.5mm, the length (L) of 350mm and 700mm, and the outer diameter (Do) of 113mm was processed to have defects with $L/Do=0.5$ (56.5mm) for straight pipes and ones with $L/Do=0.25$ (28.5mm) for complex pipes, as shown in Fig.4. In addition, the part where the transverse center line of the defect in the circumferential direction was horizontal to the infrared camera was changed to 0° as shown in Fig.4 (b), and the defect depth was regularly changed according to the pipe thickness, as shown in Table 4 below.



(a) pipe according to circumferential direction

(b) pipe according to wall-thinning depth

Figure 4. Dimensions of defects in pipe

Table 3. Dimensions of the specimen and wall-thinning defect

Specimen	Pipe Type	Thinning Depth (d/t)	Thinning Length (L/D_1)	Thinning Angle (θ/π)
700 mm				
	straight(a)	0.75, 0.25, 0.5, 0.25	0.25	0.25
	straight(b)	0.5	0.5	0.25
350 mm				
	straight	0.75, 0.5, 0.75, 0.5, 0.75	0.25	0.25
Complex (angle, 350 mm)				
	straight	0.75, 0.5, 0.25	0.5	0.25
	elbow	0.25, 0.5	0.25, 0.5	0.125, 0.25

3. Experiment Methods

Three types of pipes with processed defects were cooled using a cooling device. At this time, in order to prevent light from reflecting, radiation paint (KRYLON 4290 Ultra Flat Black) was applied to the object to keep its emissivity up to 0.97. Furthermore, temperature around the experiment system was kept constant at 25°C during the experiment. The IRT camera (FILR SC 5200) was used to measure the surface of the pipes and image data were obtained and analyzed from phases and amplitudes measured. The experiment was conducted at the pipe temperature set to 250°C or higher, under the condition derived for the purpose of this present, and with the distance of 1.5m between the IRD camera and the cooling device. Specifications of the piping loop system and those of the cooling device are as follows:

4. Experiment Methods

Using cooling unit onto heated pipe, defect image can be obtained, and detailed experimental results for phase lock-in are listed in Table 4. Corresponding graph and image can confirm the defect. Overall image and lock-in IR image profile according to defect condition can confirm the temperature distribution as shown in Table 5. By differentiation of temperature profile, results of Table 7 can be obtained. Meanwhile, distance between defect is assumed to be distance between two inflections. From whole data in Table 5, the closest data are extracted to Table 6, and those data are differentiated to extract the final results. On Table 6, results out of different defect depth and lengths are shown, and Table 11 are the results out of differentiation. On Table 8, temperature distribution and wall thinning is shown according to different defect length. Table 9 shows the results for change in wall thinning depth and temperature distribution according to defect length using lock-in IR thermography. From these results, conventional IR thermography shows 15.54% of error, but 5.31% of error is reported in lock-in IR thermography. In addition, image collected from lock-in IR thermography is more vivid than the one from conventional IR image. By summarizing all these results, change in defect length and wall thinning depth can be identified with lock-in IR thermography.

Table 4. Thermography and lock-in thermography image

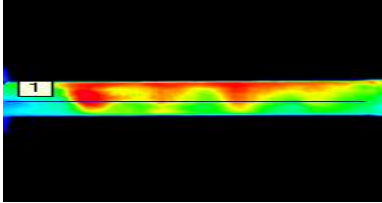
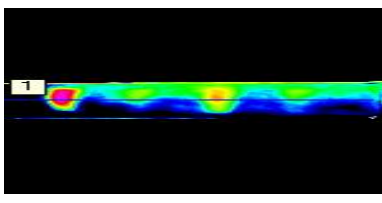
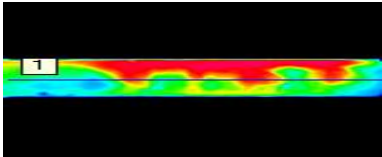
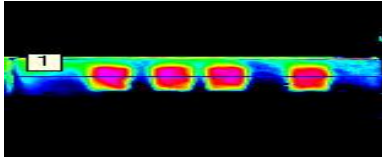
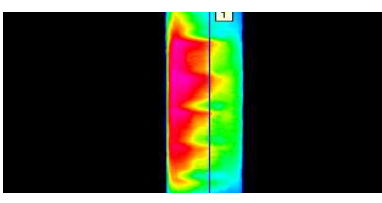
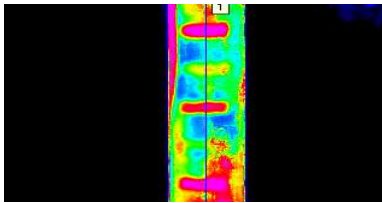
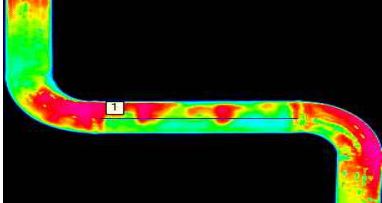
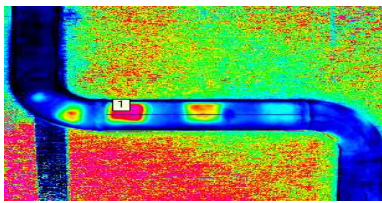


Specimen	Pipe Type	Thermography Image	Lock-in Thermography Image
700 mm	straight(a)		
	straight(b)		
350 mm	straight		
Complex (angle, 350 mm)	straight		
	elbow		

Table 5. Thermography and lock-in thermography temperature graph

Specimen	Pipe Type	Thermography Image	Lock-in Thermography Image
700mm	straight(a)		
	straight(b)		
350mm	straight		
Complex (angle, 350mm)	straight		
	elbow		

Table 6. Thermography and lock-in thermography temperature depth graph

Specimen	Pipe Type	Thermography Image	Lock-in Thermography Image
700mm	straight(a)	<p>Graph showing Temperature (°C) vs Pixel for 75% (black squares), 50% (red circles), and 25% (blue triangles) penetration depths. The 75% depth shows the highest temperature peak (~185°C) at pixel 10, while the 25% depth shows the lowest peak (~180°C) at pixel 10.</p>	<p>Graph showing Digital level (ΔT) vs Pixel for 75% (black squares), 50% (red circles), and 25% (blue triangles) penetration depths. The 75% depth shows the highest digital level peak (~26) at pixel 10, while the 25% depth shows the lowest peak (~11) at pixel 10.</p>
	straight(b)	<p>Graph showing Temperature (°C) vs Pixel for 50% penetration depth (black squares). The temperature peaks at approximately 183°C at pixel 15.</p>	<p>Graph showing Digital level (ΔT) vs Pixel for 50% penetration depth (black squares). The digital level peaks at approximately 27 at pixel 15.</p>
350mm	straight	<p>Graph showing Temperature (°C) vs Pixel for 75% (black squares) and 50% (red circles) penetration depths. The 75% depth peaks at ~209°C at pixel 15, while the 50% depth peaks at ~207°C at pixel 15.</p>	<p>Graph showing Digital level (ΔT) vs Pixel for 75% (black squares) and 50% (red circles) penetration depths. The 75% depth peaks at ~44 at pixel 30, while the 50% depth peaks at ~25 at pixel 30.</p>
Complex (angle, 350mm)	straight	<p>Graph showing Temperature (°C) vs Pixel for 75% (black squares), 50% (red circles), and 25% (blue triangles) penetration depths. The 75% depth peaks at ~235°C at pixel 15, while the 25% depth peaks at ~218°C at pixel 15.</p>	<p>Graph showing Digital level (ΔT) vs Pixel for 75% (black squares), 50% (red circles), and 25% (blue triangles) penetration depths. The 75% depth peaks at ~55 at pixel 30, while the 25% depth peaks at ~22 at pixel 30.</p>

Table 7. Thermography and lock-in thermography differential graph

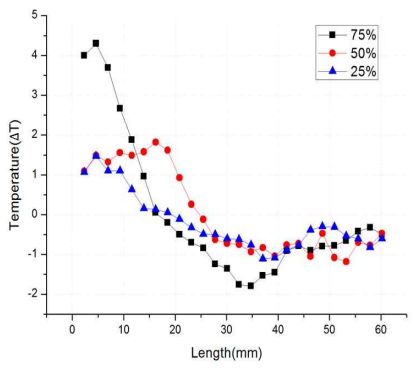
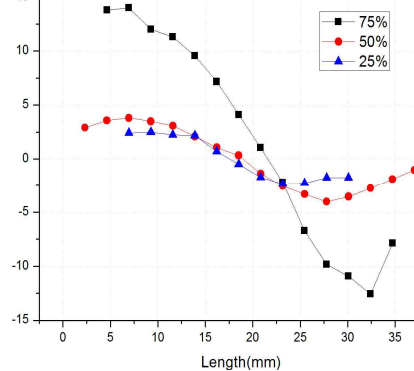
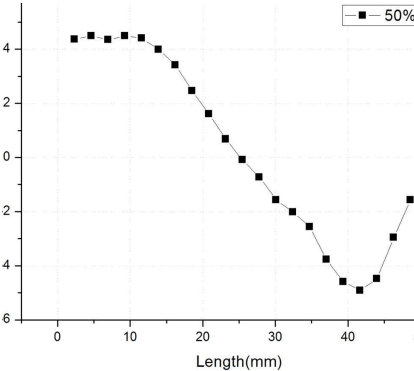
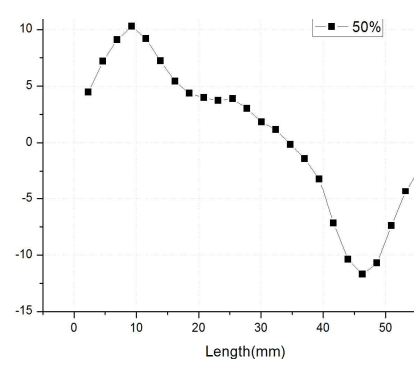
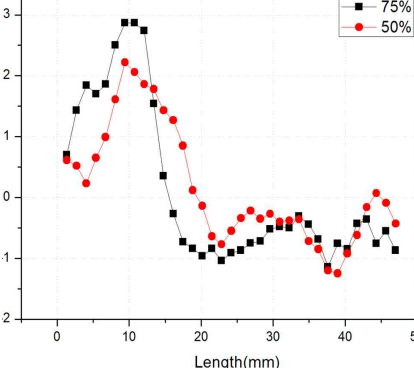
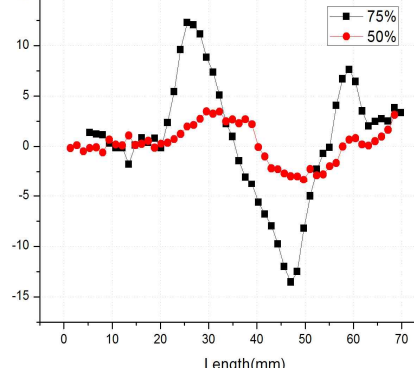
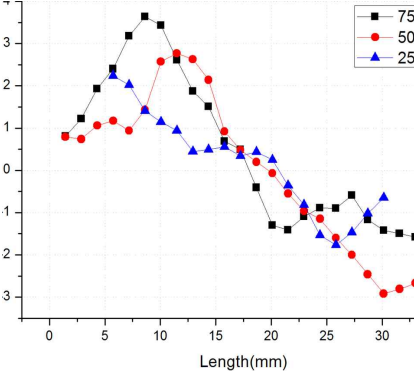
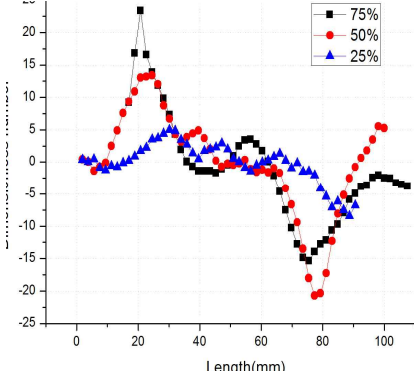
Specimen	Pipe Type	Thermography Image	Lock-in Thermography Image
700mm	straight(a)		
	straight(b)		
350mm	straight		
Complex (angle, 350mm)	straight		

Table 8. Lock-in thermography defect length(mm)

Specimen	Pipe Type	Thinning Depth	Defect length	Measuring efficiency
700mm	straight(a)	75%	29.52	3.58%
		50%	26.84	5.82%
		25%	25.58	10.25%
	straight(b)	50%	53.05	6.11%
350mm	straight	75%	27.16	4.70%
		50%	26.56	6.81%
Complex (angle, 350mm)	straight	75%	54.72	3.15%
		50%	54.52	3.50%
		25%	58.69	3.88%
Average(%)				5.31%

Table 9. Thermography defect length(mm)

Specimen	Pipe Type	Thinning Depth	Defect length	Measuring efficiency
700mm	straight(a)	75%	30.10	5.61%
		50%	23.15	18.77%
		25%	32.42	13.75%
	straight(b)	50%	45.42	19.61%
350mm	straight	75%	23.44	17.75%
		50%	23.44	17.75%
Complex (angle, 350mm)	straight	75%	48.40	14.34%
		50%	48.66	13.88%
		25%	46.10	13.41%
Average(%)				15.54%

5. Conclusion

In this study, the following conclusions were obtained:

- 1) At 1.5 m of measurement distance for different defect length and wall thinning depth, conventional IR image has 15.54% of error, meanwhile, lock-in IR thermography reported 5.31%.
- 2) Lock-in IR thermography is more precise when depth of defect is deeper, which is contradictory for conventional IR thermography.
- 3) Results from this study can be used as fundamental background for confirming the location of defect using cooling unit.

REFERENCES

- [1] Y. M. Cheong, "Experimental evidence and analysis of a mode conversion of guided wave using magnetostrictive strip transducer," *Journal of the Korean Society for Nondestructive Testing*, Vol. 29, No. 2, pp. 93-97 (2009)
- [2] M. Y. Choi and W. T. Kim, "The utilization of nondestructive testing and defects diagnosis using infrared thermography," *Journal of the Korean Society for Nondestructive Testing*, Vol. 24, No. 5, pp. 525-531 (2004)
- [3] Korea Hydro & Nuclear Power Co., "Management program for thinned pipe in NPP secondary system," Final Report-00NJ12 (2003)
- [4] S. H. Lee, T. R. Kim, S. C. Jeon and K. M. Hwang, "Thinned pipe management program of Korean NPPs," *Transaction of SMiRT-17*, Paper #O04-2, Prague, Czech Republic (2003)
- [5] IAEA, "Development of protocols for corrosion and deposits evaluation in pipes by radiography," *IAEA-TECDOC-1445* (2005)
- [6] T. Knook, M. Persoz, S. Trevin, S. Friol, M. Moutrille and L. Dejoux, "Pipe wall thinning management at Electricite de France (EDF)," *E-Journal of the Advanced Maintenance*, Vol. 2, pp. 1-13 (2010)
- [7] K. J. Lee, H. S. Jang, H. C. Jung and K. S. Kim, "Quantitative out-of-plane deformation measurement of pressure vessel with the defect using shearography," *Journal of the Korean Society for Precision Engineering*, Vol. 23, No. 10, pp. 36-42 (2006)
- [8] X. P. V. Maldague, "Trends in Optical Nondestructive Testing and Inspection," P. K. Rastogi, Elsevier Science, Switzerland (2000)
- [9] O. Breitenstein and M. Langenkamp, "Lock-in Thermography," Springer, Germany, pp. 1-38, (2003)
- [10] J. H. Park, M. Y. Choi and W. T. Kim, "Shearing phase lock-in infrared thermography for defects evaluation of metallic specimen," *Journal of the Korean Society for Nondestructive Testing*, Vol. 30, No. 2, pp. 91-97, (2010)